Development of ultrawide range viscometer and its application to boro-silicate glasses and melts.

Yutaka SHIRAISHI, Seizo NAGASAKI
and Michiyasu YAMASHIRO.
AGNE Gijutsu Center Ltd.,
Minami-aoyama 5-1-25, Kitamura Bld.
Minato-ku, Tokyo, 107, Japan.
Phone:+81 3-3409-5329,Fax:+81 3-3409-8237

ABSTRUCT

In order to measure the viscosity from glassy to molten states as a function of temperature, an ultrawide range viscometer has been developed based on a combination of the indentation, parallel-plate and rotating plate methods. A cylindrical sample with a small ball is sandwiched between the parallel plates and pressed by a suitable load and its deformation rate is measured under an operation of ascending temperature process. After the ball penetrated into the sample, bulky creep of the sample is followed. When the sample is melted, the lower plate is rotated and the torque generated on the upper plate is measured. Thus, a wide range of viscosity, $10^{12} \sim 10^{1}$ Pa·s, can be determined. After the reliability of the viscometer was confirmed using boron trioxide, the viscosity of $Na_2O \cdot 2SiO_2 - B_2O_3$ system was measured in both glassy and molten states.

1. INTRODUCTION

Most traditional method for making glass is a fusion process in which glass forming materials are frozen from the molten state via supercooled liquid. The structure of glass thus obtained is almost the same as that of liquid[1] and the essential difference between glass and liquid is in the difference of the mobility of the costituent species[2]. As schematically shown in Fig.1, the viscosity of glass forming materials is in the order of $10^{1} \sim 10^{3}$ Pa·s at their molten state and increases monotonously during the cooling and finally tends to about 10^{13} Pa·s at their glass transition point at which the translational and rotational freedoms of atoms are lost. Thus, it is necessary to develope a wide range viscometer extending to a 10^{10} Pa·s range for tracing of glass forming or glass melting processes[3].

From the practical point of view, there are many important problems relating to the viscosity of glass - exactly speaking, the viscosity of glassy materials in supercooling state. For example, the viscosity is important factor in the following processes ; such as, the annealing of glass, glass blowing, lubrication of extrusion process, and melting practice of glass. For these purposes, there are several temperatures are specified to indicate the characterized the viscosity as shown in Fig.1. On the other hand, an apparent activation energy of viscous flow is quite different in the glassy and the molten states[4]. This fact suggests the different mechanism of viscous flow prevails in the glassy and the molten states. To elusidate the change of flow mechanism between glassy and molten states, the developement of wide range viscometer is useful. In this paper the developed wide range viscometer and its application to the borosilicate system are described.

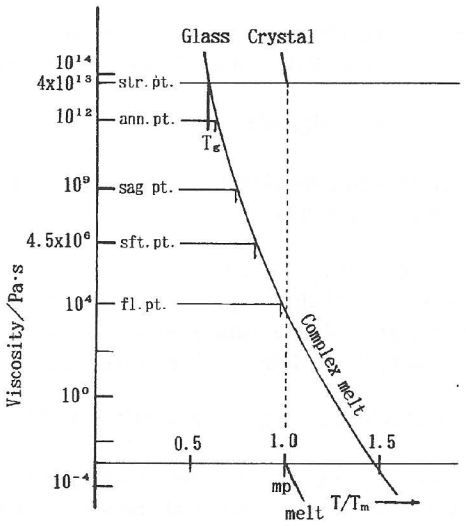

Fig. 1 Schematic diagram of glass viscosity as a function of the temperature reduced by melting point.

2. EXPERIMENTS

2.1 Measuring method

The newly developed viscometer is based on the combination of three methods. Namely,(1) indentation method,(2) parallel plate method, and (3) rotating plate method are used sequentially from glassy to molten states as shown in Fig.2. Firstly, brief descriptions are given for these methods.

(1) Indentation method

According to Douglas et al.[5], when a small sphere, radius r/m, penatrates into a glass body under a pressure, M/kg, the indentation length, l/m, during time, t/s is related with the viscosity of glass, η/Pa·s, by

$$\eta = (9/32)(Mgt/(2r)^{1/2} l^{3/2}), \quad (1)$$

where g is the acceleration of gravity, 9.807 $m \cdot s^{-2}$. Then, the indentation rate, dl/dt, is related with the viscosity as

$$\eta = (3/16) \cdot (Mg/(2rl)^{1/2}(dl/dt)). \quad (2)$$

In this experiment, a small ball, 2mm diameter, on a disc is used as shown in Fig.2(1).

(2) Parallel plate creep method

When a cylindrical glass sample placed between two plates is pressed by a suitable weight, M/kg, the creep rate of the sample, $dH/dt/m \cdot s^{-1}$, is expressed as,

$$-(dH/dt) = (2\pi H^5 Mg/3\eta V^2) + (H^2 Mg/3\eta V), \quad (3)$$

where H/m is a height of the sample whose viscosity is η/Pa · s and V/m^3 is a volume of the sample which is assumed as non－compressible Newtonian fluid. The first term given by Gent[6] corresponds to spreading of the sample and the second term added by Fontana[7] causes by collapse of the sample. This method is applied to the present viscometer for covering of the viscosity range from 10^8 to 10^5 as shown in Fig.2(2).

(3) Rotating plate method

After a melting of the sample, one of the parallel plate is rotated as shown in Fig.2(3), and the exerted torque on the other plate by a drag of the molten sample is measured. This torque, $T_q/N \cdot m$, is calculated under the assumption of laminar flow of a Newtonian fluid as

$$T_q = 2\pi \eta \omega r_0^4/4d \quad (4)$$

where ω/rad · s^{-1} is a angular velocity of the rotating plate, r_0/m is a radius of the sample liquid and d/m is a distance (gap) between two plates. In this experiment, lower plate is rotated and upper plate is used as a detector of the torque. If we introduce the volume of the sample, V/m^3, instead of r_0, then the viscosity can be written as,

$$\eta = 2\pi d^3 T_q/\omega V^2 = d^3 T_q/V^2 N \quad (5)$$

where N is a revolution speed per second.

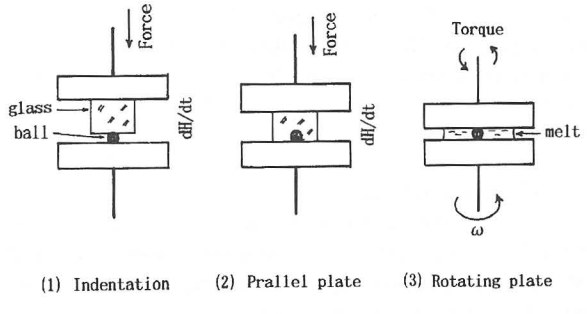

Fig. 2 Schematic illustration of measuring methods.

2.2 Apparatus and preliminary test

After several trials of the rotating plate method, the apparatus shown in Fig.3 has been made. The apparatus consists of three parts, i.e. a sensing part, a rotary part and a furnace. The upper part from the sample has sensing devices to measure the height of the sample and the torque exerted on the sensing disc. A displacement transducer (LVDT) serves to detect the sample height and two load cells are used for measurment of torque. Load cells are tied to each other by polyester thread via a pulley fixed to the sensing shaft. Weight holder with a removal mechanism is also fixed to the sensing shaft. The lower part from the sample has a rotary mechanism using a servomotor with a worm gear which is fixed to the rotary shaft. They are mounted on an elevator for adjusting the position of the rotary disc. To maintain an inert atmosphere around the sample, Ar gas containing a small amount of hydrogen is introduced from a center of a reaction tube, 35mm I.D. × 220 mm long, fixed to the inside of a SiC furnace. Lower end of the reaction tube is plugged by an alumina fiber brick with a packing device using asbestos cord for a pierce of the rotary shaft. Upper opening of the reaction tube is narrowed by a long alumina collar to minimize penetration of outer atmosphere. Alumina tubes, 5 mm I.D. × 8 mm O.D., are used for the sensing and rotary shafts. Stainless steel, 18/8, is used for discs.

Figure 4 shows a block diagram of the data signals

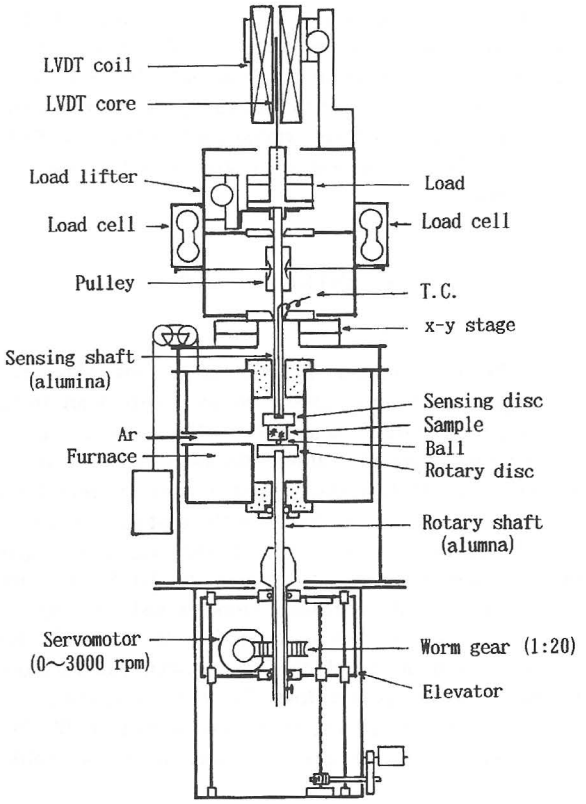

Fig. 3 Schematic diagram of the viscometer.

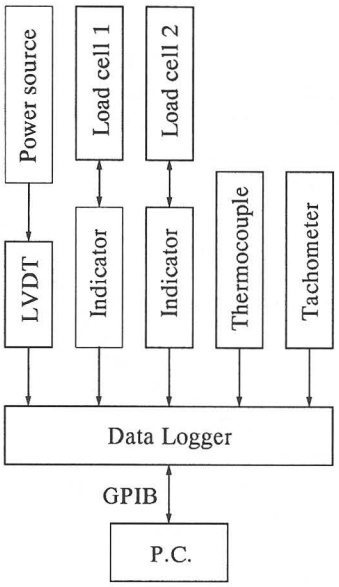

Fig. 4 Block diagram of data signal processing.

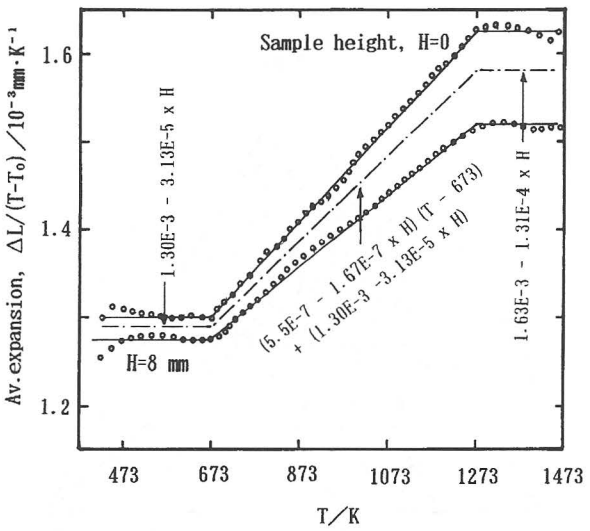

Fig. 5 Average thermal expansion of aparatus using alumina shafts.

processing system. All the signals from the viscometer — i.e. the output of LVDT, thermocouple, load cells and tachometer — are inputted to a data logger at a suitable time interval and processed by a personal computer on real time.

Most important point for a preliminary test is in the correction of thermal expansion of the apparatus. Since the height of the sample is a basic quantity from which the viscosity in glassy state is calculated, an accurate value of the overall thermal expansion of the apparatus is necessary for the correction. Since the expansion of the apparatus is affected by many experimental conditions, e.g. materials and geometry of the shafts, nature of a thermal insulator in the furnace, temperature and heating rate, and so on, thus, the correction factor should be determined under the same condition as that of the actual measurement. Example of the thermal expansion from which the correction factor was obtained is shown in Fig.5. For a real calibration of the sample height, the correction of the expansion should be observed as a function of the temperature and the sample height, at least. However, since all the cases can not be carried out, two extreme cases, which correspond to zero and initial sample height, were measured precisely. The results were reproduced well above 670 K. Then, the empirical calibration equation for a thermal expansion was derived under an assumption of a linear dependency of the sample height. Since the lowest temperature in the actual measurements was 730 K, then the correction for the thermal expansion was adequatly performed on the viscosity calculation.

Next point is to get an empirical equation for viscosity measurement instead of the theoretically derived equation. The theoretical equation (5) requests the torque caused by a drag force of the sample at unit revolution speed. However, it is difficult to measure this torque absolutely, because our sensing system of the torque has a finite amount of a moment of inertia which inevitably causes an additional force to the detecting torque. Thus, for the proper use of the equation (5), it is necessary to know the exact dependence of the torque on the rotational speed separated from the effect of the moment of inertia. For this purpose, three to five levels of measurements varying the rotational speeds are required. On the other hand, since the viscosity violently changes with temperatures in the melting range, a rapid measurment is preferable, especially in an ascending temperature condition which is adopted in this experiment. Thus, we have chosen the use of an empirical equation for determination of the viscosity value from a measurement of single revolution speed. Using four kinds of standard reference oil for viscosity, an empirical equation (6) was obtained as a resultant of linear regression between torque, revolution speed, and the viscosity.

$$\eta = (6.41 \times 10^3 T_q/N) - (0.101/N) \qquad (6)$$

where, η , T_q, and N are expressed in Pa · s, N · m, and min^{-1}, respectively.

2.3 Samples

The composition of the samples used in this experiment is shown in Fig.6 by circles. Starting materials of all these samples were special grade chemicals of sodium carbonate anhydrous, silicon dioxide and boron trioxide powders. To make a glass of boron trioxide, powder was fused in a Pt crucible at 1070 K and poured onto a metal plate after bubbling had ceased. Sodium disilicate mother glass was prepared by almost similar way but melted at 1470 K. Both glasses were mixed to make desired composition and melted in a Pt crucible and

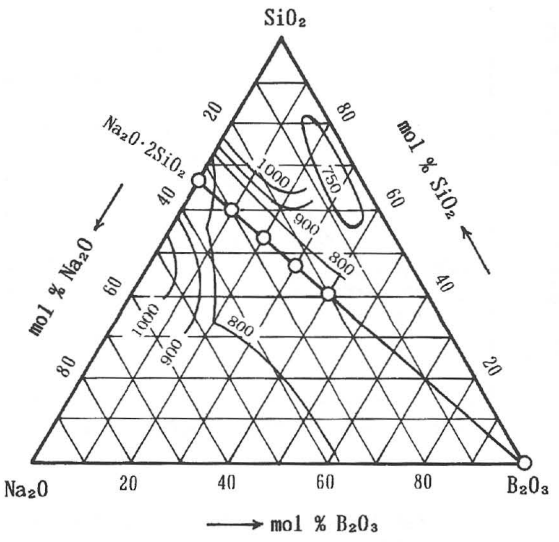

Fig. 6 Composition of the samples.

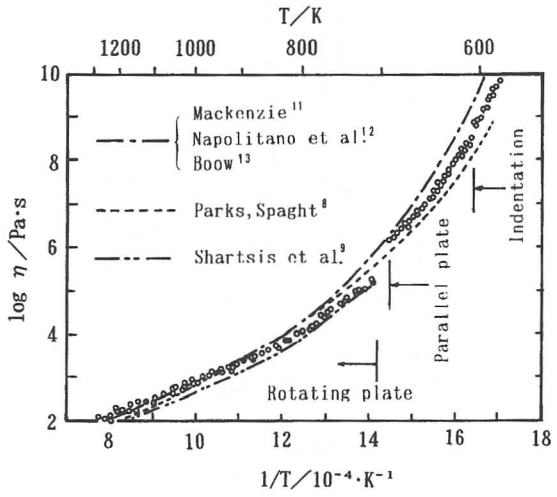

Fig. 7 Viscosity of B_2O_3. Results of three independent heats are plotted together.

casted into a graphite mould, 12 mm I.D, keeping at about 700 K and held at that temperature for more than one hour to anneal the cast. After annealing, ingot was cut and polished to several pieces having a length, about 6 mm, and was surved for measurement.

2.4 Experimental procedure

Outline of the experimental procedure is as follows: At first, the rotary disc is set up so as to minimize a deflection of the rotation, ususally less than 0.5 mm. Next, a ball is put on a hollow of the rotary disc and measure a gap between the parallel plate. Then, the sample, whose geometry was measured thoroughly by a micrometer, is placed on the ball and settled by the sensing disc. The furnace is moved to the right position and heated at a specified heating rate under Ar atmosphere.

It can be observed that the sample expands during the heating and then begins to deform when temperature reached near the glass transition temperature, T_g. Average thermal expansion coefficient can be calculated at T_g from the observed amount of expansion. When the contraction of the sample height is observed, the viscosity of the sample is calculated by Eq.(2) with a consecutive sampling of the indentation depth. After the indentation of the ball has been done, the parallel plate creep follows immediately and the viscosity is calculated by Eq.(3). The value of viscosity, based on the measurement of the creep rate and height of the sample, gradually decreases with the increase of temperatures untill the sample height reaches to the ball gap height between two plates. The melting temperature is defined under the criterion that the sample height reached to the height of the gap and ceased further decrease. Above the melting temperature, viscosity measurement are carried out by a manual control of the revolution speed to obtain the suitable amount of the generated torque. After the run, solidified shape of the sample on the rotary disc was observed to judge the experimental condition.

3. RESULTS AND DISCUSSION

3.1 B_2O_3

Figure 7 shows the viscosity of B_2O_3 as a function of temperature. The results measured by three independent heats are plotted together. There can be observed a small gap or leap at a joint of the measuring methods. Discontinuity between the indentation and parallel plate methods may be attributed to a precision of the sample shape and that of the parallel plate to the rotating plate is mostly depended on a skill of the operation. There are many previous works[8-13] which can be compared with the present work. Typical works are shown in Fig.7 by chain, dotted and double dotted chain curves including a varieties of measuring method such as rotating cylinder[8, 10, 12], counter - balanced sphere[9, 11], and penetration methods[13]. The agreement is enough to prove the validity of the viscometer developed here.

3.2 Pseudo - binary system of $Na_2O \cdot 2SiO_2 - B_2O_3$

There are not so many previous works on the viscosity of this pseudo - binary system except $Na_2O \cdot 2SiO_2$. Figure 8 shows the viscosity of $Na_2O \cdot 2SiO_2$ as a function of temperature and Table 1 gives the comparison with previous works[14]. Though there are no measured data for comparison in the mid range of the viscosity, the agreement is also reasonable in both glassy and molten

Table 1 Viscosity of sodium disilicate[14].

composition	log Viscosity / Pa · s at Temperature K											
mole % Na2O	695	711	767	833	880	1073	1173	1273	1373	1473	Author	Remark
33	14.0	13.0									Suzuki	Beam bend
$Na_2O \cdot 2SiO_2$			9.0	7.0	6.0						Matsusita	Beam bend
33.3						3.44	2.70	2.08	1.58	1.20	Skornyakov	Rot. sphere
33.1						2.89	2.10	1.50	1.05	0.70	Eipeltauer	Count. bal.
$Na_2O \cdot 2SiO_2$							2.45	1.82	1.35	0.92	Prestion	Rot. cylind.
33.1							2.71	2.08	1.58	1.18	Lillie	Rot. cylind.
32.9							2.66	2.08	1.57	1.18	Shartsis	Count. bal.
33.6							2.76	2.11	1.56	1.13	Shvaiko-Shvaikovskaya	Count. bal.
$Na_2O \cdot 2SiO_2$								2.12	1.65	1.25	Sasek	Penetration
33.0									1.55	1.13	Bockris	Rot. cylind.
$Na_2O{\bullet}2SiO_2$			8.9	6.7	5.7	3.24	2.55	2.06	1.68	1.38	This work	P. P. creep / rot

Table 2 Fulcher parameters and calculated viscosity of $Na_2O \cdot 2SiO - B_2O_3$ system.

Composition / mol%		log η / Pa · s at temperature /K				Parameter			fitting range	
$Na_2O \cdot 2SiO_2 - B_2O_3$		800	1000	1200	1400	A	B	T_0	T / K	$\sigma \times 10^3$
100	0	7.70	3.92	2.41	1.59	− 1.127	2356	533.1	737 − 1477	625
			【4.54	2.96		− 0.722	2443	536.4	805 − 1438】[15]	
90	10	9.44	3.53	1.97	1.26	− 0.684	1442	657.6	808 − 1283	94
80	20		3.54	1.67	0.85	− 1.231	1478	690.5	835 − 1293	129
			【4.19	1.90		− 2.273	2352	636.3	857 − 1422】	
70	30		3.63	1.80	1.07	− 0.618	1125	735.1	841 − 1336	266
			【4.163	1.67		− 2.866	2544	638.0	887 − 1416】	
60	40	10.29	3.31	1.39	0.49	− 1.990	1866	648.0	809 − 1243	211
			【4.077	1.55		− 2.982	2525	642.3	887 − 1416】	

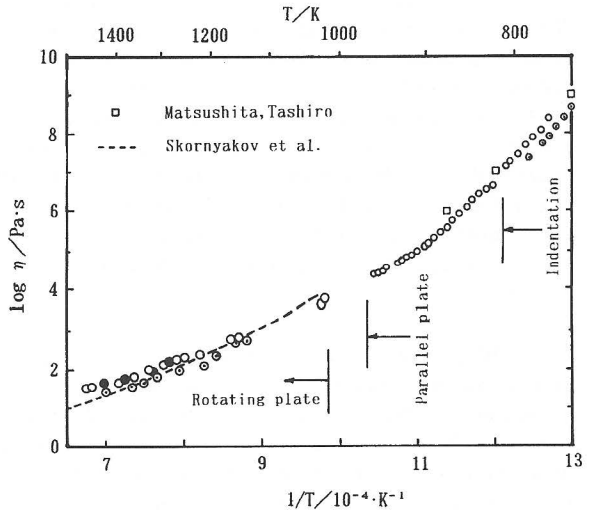

Fig. 8 Viscosity of $Na_2O \cdot 2SiO_2$. Results of two separate heats are indicated by the marks ○ and ◉ , respectively. Solid circles indicate the cooling data followed the heating process of open circles.

states except in higher temperature region. Our previous data[15], which is obtained by an interpolation from the independent measurements of glass and the melt, shows a little higher value than the present result due to a lack of the mid range data of the viscosity.

The measured viscosities of this system were well represented by the Fulcher function, $\log\eta = A + B/(T - T_0)$. Fitted parameters, A, B and T_0 are listed in Table 2 comparing with the previously determined[15]. Fitted curves using these parameters are given in Fig.9 as a function of temperature. As can be seen in Fig.8, the relation between the viscosity and the B_2O_3 content is reversed in glassy and molten states. Namely, in the glassy state, the viscosity increases with the increase of the B_2O_3 content but it decreases in molten state. This behaviour is more clearly shown in the isoviscosity curves in Fig.10, in which the liquidus line is also included. It is evident from Fig.10 that the effect of boron oxide changes around 30 mol % of B_2O_3 content. As it is well knwon by NMR study of borosilicate glass[16] that boron atom takes a four fold coordination of oxygen and participates a tetrahedral net work in silicate glass when the excess oxygen to form a tetrahedral coordination is available. In the present case, the increase of glass viscosity till 30 mol % would be interpreted by the

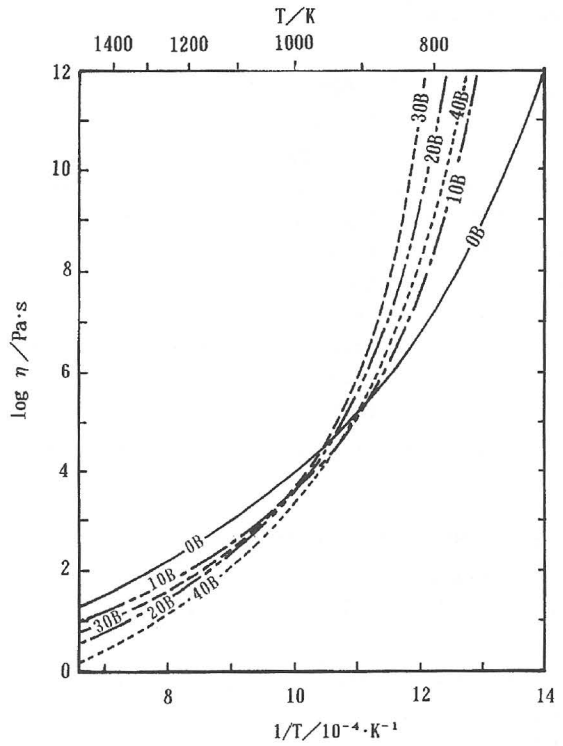

Fig. 9 Viscosity of $(1-x)Na_2O \cdot SiO_2 - xB_2O_3$ system, where x denotes mol % B_2O_3. Curves are drawn by Fulcher function using the parameters given in Table 2.

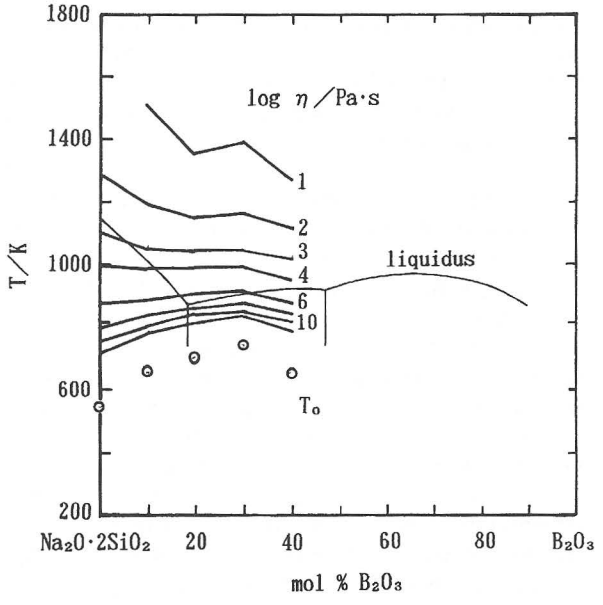

Fig. 10 Isoviscosity curves of $Na_2O \cdot SiO_2 - B_2O_3$ system. Where T_0 indicates a hypothetical temperature at which viscosity tends to infinit in Fulcher function.

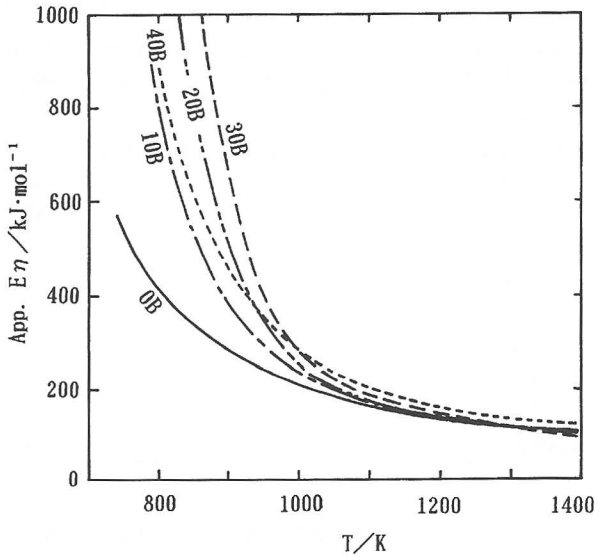

Fig. 11 Apparent activation energy E_η for viscous flow in $(1-x)Na_2O \cdot SiO_2 - xB_2O_3$ system, where x denotes mol% B_2O_3. Values of E_η are obtained from the tangents to the curves in Fig.9 at any temperature.

developement of the network due to the increase of the boron atoms coordinated to four oxygen atoms. And further addition of boron oxide creates the three oxygen coordinated boron atoms and tends to a degradation of the tetrahedral network and thus, the viscosity decreases.

Figure 11 shows the apparent activation energy of viscous flow as a function of temperature. Here, the apparent activation energy is determined by the tangent to the curves given in Fig.9 at any temperature. Huge difference of the activation energy can be seen between glassy and molten states. This fact seems to be suggested that the quite different mechanism of viscous flow prevails in glass and the melt. As it is well known that the spatial arrangement of atoms in glass and the melt is quite similar to each other and the fundamental difference between them is in a fluctuation of the structure, i.e. the position of the atoms moves from time to time in the molten state but it does not change so easily even in the supercooling state of glass.

When boron atom is introduced into the silicate network as an oxygen four fold coordianted atom, it may participates to form a tetrahedral network. Though an addition of boron atoms would be caused an development of the network, but the boron atom simaltaneously brings some distortion into the network due to the differnce in the ionic charge and the bond length and so on. So, the stiffness of the network would be lost by the addition of boron atoms even though the size of network is still developed. When a shear flow is occured, a flow unit of the network should be jumped one poition to another. Easiness of this jump would be depended on the size and

the deformability of the flow unit. In the glassy state, the flow unit of the network has little fluctuation to deform the shape. On the other hand, in the molten state, deformation of the flow unit is relatively easy due to the larger fluctuation of a structure. These two factors, size and deformability, and the difference of a structural fluctuation might be able to explain the opposit behaviour of boron oxide added to borosilicate in glassy and molten states.

Of course, there is no evidence to proof this speculation in this moment. However, this opposit behaviour of boron atom is quite interest and should be gave much deeper understanding of flow mechanism in glassy and molten states. If we would be able to provide the condition in which the fluctuation time is comparable to the experimental time scale, we would have more information to clarify the phenomena.

4. CONCLUSION

(1) An ultrawide range viscometer was developed based on a combination of the indentation, parallel plate, and rotating plate methods.

(2) Developed viscometer can be operated well to cover a viscosity range from 10^{12} to 10^{1} Pa · s. Reliability of the viscometer was tested by the measurement, covering from glassy to molten states, of boron trioxide up to 1473 K.

(3) Viscosity of pseudo-binary $Na_2O \cdot 2SiO_2$-B_2O_3 system has been measured from glassy to molten states. It was observed that the viscosity increses with increase of B_2O_3 content in glassy state, but it decreases in molten state. This unusual behaviour would be interpleted by the terms of a deformable network and a fluctuation of the structure.

REFERENCES

1. See for example, Y. Waseda, *Chemical Properties of Molten Slags*, Ed. by S.Banya and M. Hino, Iron and Steel Inst. Japan, 1991, pp 243-265.
2. Y. Shiraishi, Kinzoku, Vol.64, No.12, 1994, p.2.
3. Y. Shiraishi, S. Nagasaki and M. Yamashiro, Nihon Kinzoku Gakkai-shi, Vol.60, 1996, p.184.
4. Y. Shiraishi and H. Ogawa, Tohoku Daigaku Senken Iho, Vol.44, No.1, 1988, p.8.
5. R. W. Douglas, W. L. Armstrong, J. P. Edward and D. Hall, Glass Tech., Vol.6, 1965, p.52.
6. A. N. Gent, J. Appl. Phys., Vol.17, 1946,p.458.
7. E. H. Fontana, Amer. Ceram. Soc. Bull., Vol.49, 1970, p.594.
8. G. S. Parks and M. E. Spaght, Physics, Vol.6, 1935, p.69.
9. L. Shartsis, W. Capps and S. Spinner, J Amer. Ceram. Soc., Vol.36, 1953, p.319.
10. A. Dietzel and R.Blückner, Glasstech. Ber., Vol.28, 1955, p.455.
11. J. D. Mackenzie, J. Phys. Chem., Vol.63, 1959, p.1875.
12. A. Napolitano, P. B. Macedo and E. G. Haukins, J. Amer. Ceram. Soc., Vol.48, 1965, p.613.
13. J. Boow, Phy. Chem. Glasses, Vol.8, 1967, p.45,
14. O. V. Mazurin, M. V. Streltsina and T. P. Shvaiko-Shvaikovskaya, *Handbook of Glass Data*, Part (A), Elsvier, 1983, pp.271-293.
15. Y. Shiraishi and H. Ogawa, Proc. 3rd. Intern. Conf. on Molten Slags and Fluxes, Glasgow, U. K., The Instit. of Metals, 1989, p.190.
16. M. Imaoka, H. Hasegawa, A. Hamaguchi and H. Kurotaki, Yogyo Kyokai-shi, Vol.79, 1971, p.164.